RSC Advances

PAPER

View Article Online
View Journal | View Issue

Cite this: *RSC Adv.*, 2017, **7**, 48730

Fluorescence properties of heterotrinuclear Zn(II)–M(II) (M = Ca, Sr and Ba) bis(salamo)-type complexes†

Li Wang, Xiao-Yan Li, Qing Zhao, Li-Hong Li and Wen-Kui Dong *

Received 9th August 2017
Accepted 2nd October 2017

DOI: 10.1039/c7ra08789f

rsc.li/rsc-advances

A series of hetero-trinuclear Zn(II) complexes, $[Zn_2Ca(L)(OAc)_2]\cdot CHCl_3$ (**1**), $[Zn_2Sr(L)(OAc)_2]$ (**2**) and $[Zn_2Ba(L)(OAc)_2]$ (**3**) with a bis(salamo)-type tetraoxime ligand H_4L were synthesized and characterized by elemental analyses, IR, UV-vis spectra *etc.* Spectral titrations and X-ray crystallography clearly show that the stoichiometry of the heterotrinuclear complexes are all 1 : 2 : 1 (ligand/Zn(II)/M(II)). The different natures of the N_2O_2 and O_6 sites of the ligand H_4L lead to the site-selective introduction of two different kinds of metal(II) atoms. All the Zn(II) atoms are penta-coordinated with distorted square pyramidal geometries. The coordination numbers of Ca(II), Sr(II) and Ba(II) atoms in the O_6 environment are all 8, and they have slightly distorted square antiprism geometries. Furthermore, ion competitive experiments show that the coordinating capability in the central O_6 site is in the order of Ca(II) > Sr(II) > Ba(II).

1. Introduction

Transition metal complexes containing salen-type N_2O_2 ligands have received considerable attention in the past few decades,[1] because they are important materials for biological fields,[2] catalysis,[3] magnetic materials,[4] supramolecular structures,[5] luminescence,[6] electrochemical fields,[7] molecular recognition[8] and other aspects. Compared to salen-type ligands, two salicylaldehyde molecules were ligated with a bridging unit as a linker with a structural configuration (–CH=N–O–$(CH)_n$–O–N=CH–) in the structure of salamo-type ligand.[9] It can be seen that the oxygen atoms are added to a salen-type ligand, finally forming a salamo-type ligand.[10]

It is worth noting that a large number of studies have been devoted to single salamo ligands for the synthesis of single, double or multinuclear transition metal(II) complexes.[11] However, there are a few studies on bis(salamo) ligands and their complexes.[9] In this article, three heterotrinuclear complexes $[Zn_2Ca(L)(OAc)_2]\cdot CHCl_3$ (**1**), $[Zn_2Sr(L)(OAc)_2]$ (**2**) and $[Zn_2Ba(L)(OAc)_2]$ (**3**) with a naphthalenediol-based bis(salamo) ligand H_4L have been synthesized and structurally characterized. When the two salamo moieties of H_4L are metalated, six oxygen atoms are fixed in an acyclic, C-shaped arrangement.[12] The resultant 18-crown-6-like recognition site would be suitable for alkaline earth metal ion recognition. Meanwhile, a naphthalenediol ring was introduced, expected to enhance the fluorescence properties of the resultant heterotrinuclear Zn(II)–M(II) (M = Ca, Sr and Ba) complexes with the naphthalenediol-based bis(salamo)-type ligand.

2. Experimental

2.1 Materials and instruments

3-Ethoxy salicylaldehyde was purchased from Tokyo Chemical Industry and was used without further purification. Other reagents and solvents were of analytical grade supplied by Tianjin Chemical Reagent Factory. C, H and N analyses were performed by using a GmbH VarioEL V3.00 automatic elemental analysis instrument. Elemental analysis for metals was detected by an IRIS ER/S WP-1 ICP atomic emission spectrometer. FT-IR spectra were recorded on a VERTEX70 FT-IR spectrophotometer, with samples prepared as KBr (400–4000 cm^{-1}) pellets. Melting points were obtained by the use of a microscopic melting point apparatus made by the Beijing Taike Instrument Limited Company. ^1H NMR spectra were determined by a German Bruker AVANCE DRX-400 spectrometer. UV-vis absorption spectra were recorded on a Hitachi U-3900H spectrometer. Fluorescent spectra were taken on an LS-55 fluorescence photometer. X-ray single crystal structure determinations were carried out on a Bruker Smart Apex CCD diffractometer.

2.2 Syntheses of H_4L and its complexes

2.2.1 Syntheses of H_4L. The bis(salamo)-type tetraoxime ligand (H_4L) was obtained by reacting 2,3-dihydroxynaphthalene-1,4-dicarbaldehyde with 3-ethoxysalicylaldehyde, and 2,3-dihydroxynaphthalene-1,4-dicarbaldehyde was synthesized by

School of Chemical and Biological Engineering, Lanzhou Jiaotong University, Lanzhou, Gansu, 730070, P. R. China. E-mail: dongwk@126.com

† Electronic supplementary information (ESI) available. CCDC 1564434–1564436. For ESI and crystallographic data in CIF or other electronic format see DOI: 10.1039/c7ra08789f

the standard method according to the literature.[13] The synthetic route to H_4L is shown in Scheme 1. The ^1H NMR spectrum of the ligand H_4L shows clearly that it was highly symmetrical. Yield: 43.1%. Mp: 161–162 °C. Anal. calc. for $C_{34}H_{36}N_4O_{10}$ (%): C, 61.81; H, 5.49; N, 8.48. Found (%): C, 61.86; H, 5.42; N, 8.39. Selected IR bands (KBr pellet, cm^{-1}): 3391 (s), 2978 (w), 1605 (m), 1470 (s), 1257 (s), 1064 (m). ^1H NMR: δ 1.45 (s, 6H), 4.08 (s, 4H), 4.58 (s, 8H), 6.83 (s, 6H), 7.41–7.96 (dd, 4H), 8.31–9.14 (d, 4H), 9.72–11.0 (d, 4H). UV-vis [in chloroform/methanol (3 : 2)], λ_{max} (nm) [2.5×10^{-5} M]: 263, 341, 359, 378.

2.2.2 Syntheses of complexes 1, 2 and 3. A mixed solution of $Zn(OAc)_2 \cdot 2H_2O$ (5.00 mg, 0.02 mmol) and $Ca(OAc)_2 \cdot H_2O$ (1.60 mg, 0.01 mmol) in ethanol solution (3 mL) was added dropwise to a stirred solution of H_4L (3.38 mg, 0.005 mmol) in chloroform (3 mL). The yellow solution was filtered and allowed to remain in the open air for slow evaporation. The crystals of complex **1** were collected, washed with ethanol and *n*-hexane, and dried in a vacuum drying oven. Complexes **2** and **3** were prepared by a similar procedure to complex **1**.

Complex **1**, clear yellow crystals. Yield: 3.6 mg, 67.2%. Anal. calc. for $C_{39}H_{39}CaCl_3N_4O_{14}Zn_2$ (%): C, 43.99; H, 3.69; N, 5.26; Ca, 3.76; Zn, 12.28. Found (%): C, 43.82; H, 3.73; N, 5.34; Ca, 3.52; Zn, 12.26. Selected IR bands (KBr pellet, cm^{-1}): 2977 (m), 1591 (w), 1461 (m), 1317 (s), 1082 (m).

Complex **2**, dark yellow crystals. Yield: 3.0 mg, 60.8%. Anal. calc. for $C_{38}H_{38}N_4O_{14}SrZn_2$ (%): C, 45.96; H, 3.86; N, 5.64; Sr,

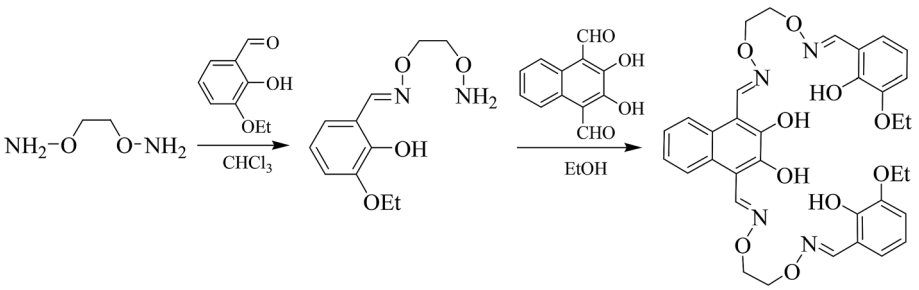

Scheme 1 Synthetic route to bis(salamo)-type tetraoxime ligand H_4L.

Table 1 Crystallographic data and refinement parameters for complexes **1**, **2** and **3**

Complex	**1**	**2**	**3**
Empirical formula	$C_{39}H_{39}CaCl_3N_4O_{14}Zn_2$	$C_{38}H_{38}SrN_4O_{14}Zn_2$	$C_{38}H_{38}BaN_4O_{14}Zn_2$
Formula weight	1064.910	993.08	1042.80
Temperature (K)	295(1)	296(2)	295(1)
Wavelength (Å)	0.71073	0.71073	0.71073
Crystal system	Triclinic	Triclinic	Triclinic
Space group	$P\bar{1}$	$P\bar{1}$	$P\bar{1}$
a (Å)	12.4374(17)	12.5470(19)	12.6093(11)
b (Å)	12.9596(18)	13.3336(19)	13.4496(12)
c (Å)	13.3757(19)	15.453(2)	15.4036(14)
α (°)	84.531(12)	111.202(5)	111.422(8)
β (°)	80.178(12)	101.075(5)	100.715(7)
γ (°)	86.928(11)	100.367(5)	99.989(7)
Volume ($Å^3$)	2113.1(5)	2275.7(6)	2304.7(4)
Z	2	2	2
Calculated density (g cm^{-3})	1.674	1.449	1.503
θ range for data collection (°)	3.268 to 26.022	2.406 to 25.499	3.410 to 26.021
F (000)	1088	1008	1044
$h/k/l$ (min, max)	−14, 15/−15, 15/−16, 15	−15, 15/−16, 16/−18, 13	−15, 15/−17, 16/−18, 19
Crystal size (mm)	033 × 0.27 × 0.25	0.28 × 0.25 × 0.22	0.27 × 0.13 × 0.10
Reflections collected	14 901/8331 [$R_{int} = 0.0606$]	17 211/8409 [$R_{int} = 0.0353$]	16 711/8995 [$R_{int} = 0.0787$]
Independent reflection	8331	8409	8995
Completeness to 26.32 (%)	99.80	99.20	99.00
Data/restraints/parameters	8331/0/572	8409/29/186	8995/0/536
Final R indices [$I > 2\sigma(I)$][a]	$R_1 = 0.0584$, w$R_2 = 0.0900$	$R_1 = 0.0665$, w$R_2 = 0.2241$	$R_1 = 0.0858$, w$R_2 = 0.2080$
R indices (all data)[b]	$R_1 = 0.1055$, w$R_2 = 0.1163$	$R_1 = 0.0875$, w$R_2 = 0.2376$	$R_1 = 0.1460$, w$R_2 = 0.2558$
Goodness-of-fit for (F^2)[c]	1.040	1.066	1.017

[a] $R_1 = \Sigma||F_o| - |F_c||/\Sigma|F_o|$. [b] $wR_2 = [\Sigma w(F_o^2 - F_c^2)^2/\Sigma w(F_o^2)^2]^{1/2}$, $w = [\sigma^2(F_o^2) + (0.0784P)^2 + 1.3233P]^{-1}$, where $P = (F_o^2 + 2F_c^2)/3$. [c] GOF $= [\Sigma w(F_o^2 - F_c^2)^2/(n_{obs} - n_{param})]^{1/2}$.

8.82; Zn, 13.17. Found (%): C, 45.98; H, 3.79; N, 5.71; Sr, 8.76; Zn, 13.24. Selected IR bands (KBr pellet, cm^{-1}): 2983 (m), 1585 (w), 1461 (m), 1317 (s), 1075 (m).

Complex **3**, clear yellow crystals. Yield: 3.4 mg, 65.3%. Anal. calc. for $C_{38}H_{38}BaN_4O_{14}Zn_2$ (%): C, 43.77; H, 3.67; N, 5.37; Ba, 13.17; Zn, 12.54. Found (%): C, 43.82; H, 3.54; N, 5.27; Ba, 13.29; Zn, 12.62. Selected IR bands (KBr pellet, cm^{-1}): 2935 (m), 1588 (w), 1457 (m), 1316 (s), 1075 (m).

2.3 X-ray crystallographic analysis

The crystallographic data for complexes **1**, **2** and **3** are summarized in Table 2. X-ray single-crystal diffraction data were collected on a graphite monochromated Mo-K_α radiation (λ = 0.71073 Å) instrument at 295(1), 296(2) and 295(1) K for complexes **1**, **2** and **3**, respectively. Complexes **1**, **2** and **3** are all crystallized in the triclinic crystal system with space group $P\bar{1}$. The structures were solved by using the program SHELXS-97 (ref. 14) and Fourier difference techniques, and refined by a full-matrix least-squares method on F^2 using SHELXL-2014.[15] H atoms were included at the calculated positions and constrained to ride on their parent atoms. The crystallographic data are summarized in Table 1. CCDC – 1564436 (**1**), 1564435 (**2**) and 1564434 (**3**) contain the supplementary crystallographic data for this article.†

3. Results and discussion

3.1 IR spectrum analysis

The obtained IR spectra show that the free ligand H_4L and its corresponding complexes **1**, **2** and **3** exhibit various bands in the region of 4000–400 cm^{-1} (Fig. 1). The O–H stretching band of the free ligand H_4L is observed at 3391 cm^{-1}. This band disappears in the spectra of complexes **1**, **2** and **3**, indicating that the phenolic and naphthalenediol hydroxyl groups of H_4L have been completely deprotonated and coordinated with the

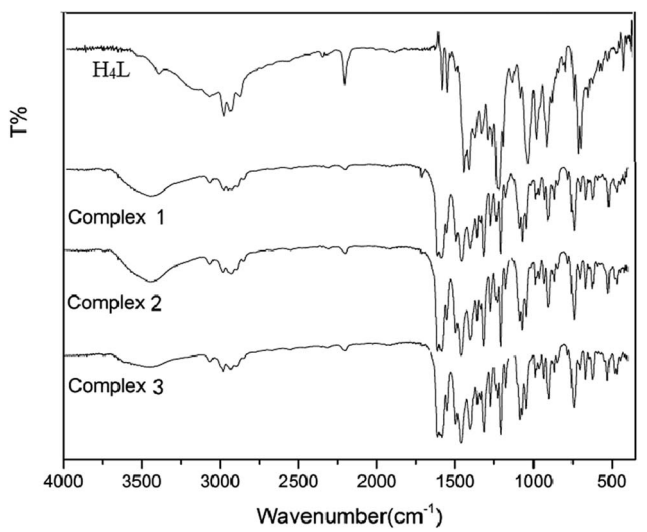

Fig. 1 IR spectra of the ligand H_4L and its corresponding complexes **1**–**3**.

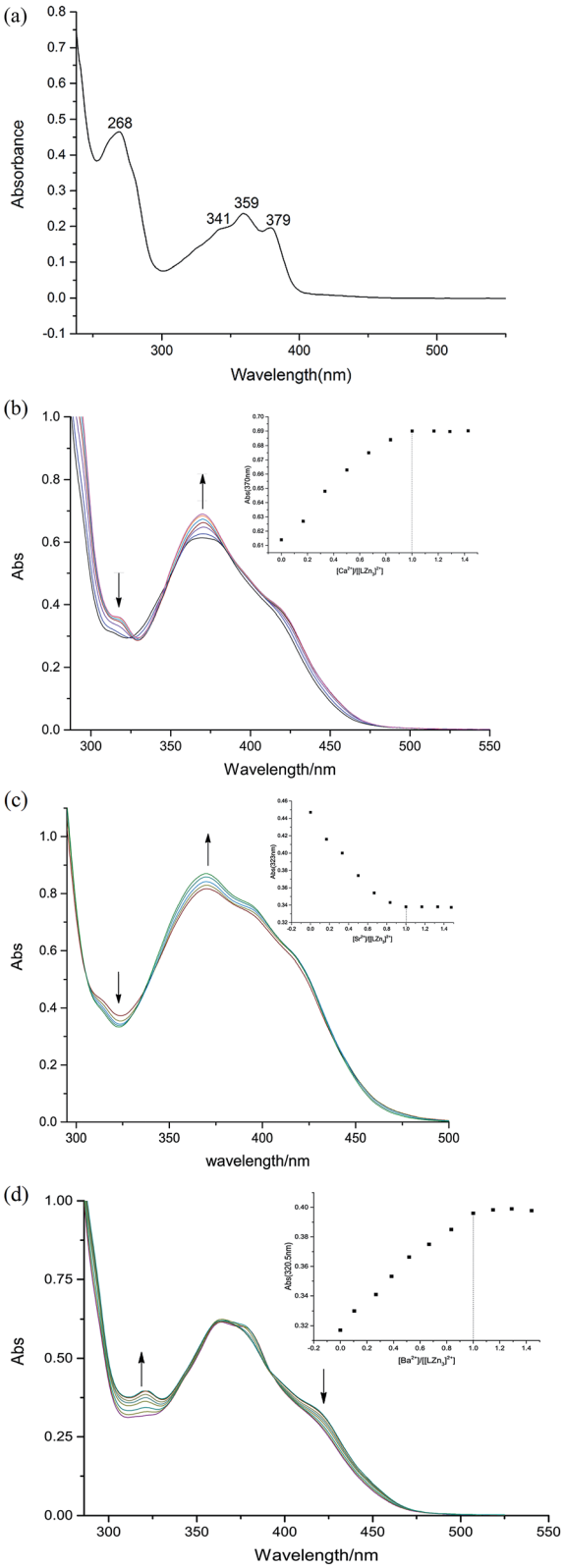

Fig. 2 (a) UV-vis spectrum of the free ligand in $CHCl_3/CH_3OH$; (b) the changes in the Zn(II)–L complex upon addition of $Ca(OAc)_2 \cdot H_2O$; (c) the changes in the Zn(II)–L complex upon addition of $Sr(OAc)_2 \cdot H_2O$; (d) the changes in the Zn(II)–L complex upon addition of $Ba(OAc)_2$.

metal atoms. The characteristic band of the C=N stretching vibration of the free ligand H_4L is located at 1605 cm^{-1}. This band is shifted by 14, 20 and 17 cm^{-1} in the low wavenumber direction in complexes **1**, **2** and **3**, indicating that the Zn(II) atoms are coordinated with the N_2O_2 atoms of the ligand.[16]

3.2 UV-vis titration spectroscopy analysis

The UV spectrum of the ligand H_4L is shown in Fig. 2(a). There are four consecutive absorption peaks at *ca.* 268, 341, 359 and 379 nm. The presence of these four peaks indicates that there is a large conjugate structure in the ligand H_4L.[17]

In the solution of chloroform : methanol (v/v = 2 : 3), the coordination ratio of the $[Zn_3(L)]^{2+}$ complex with alkaline earth metal ions was measured by UV-vis spectroscopy. ($C_{ligand} = 2.5 \times 10^{-5}$ mol L^{-1}, $C_{metal\ salt} = 1.5 \times 10^{-2}$ mol L^{-1}). The results are shown in Fig. 2(b–d).

In the titration experiments of complex **1**, the titration curves changed over two ranges. The first was in the range 360–380 nm, where the titration curves were on the rise. The second was in the range 326–303 nm, where the titration curves were decreasing, and the isoabsorptive point is at 303 nm. We selected the experimental values of the curves at 370 nm to make the concentration scale scatter plot, assuming 1 : 1 stoichiometry between Ca^{2+} and $[Zn_3(L)]^{2+}$. Similar changes also appeared in complexes **2** and **3**, which gave the same conclusions.

3.3 Description of crystal structures of complexes 1–3

The structures of the heterotrinuclear complexes **1–3** were determined by single-crystal X-ray diffraction. Selected bond lengths and angles of complexes **1–3** are listed in Table 2. The corresponding hydrogen bonds of complexes **1–3** are summarized in Table 3.

The crystal structure, atom numberings and the coordination polyhedra for Zn(II) and Ca(II) atoms in complex **1** are shown in Fig. 3. Complex **1** crystallizes in the triclinic crystal system, space group $P\bar{1}$. From the structure of complex **1**, we can see that the coordination ratio of ligand $(L)^{4-}$ to metal atoms (Zn(II) and Ca(II)) in the heteronuclear complex **1** is 1 : 2 : 1. Two Zn(II) atoms (Zn1 and Zn2) are located in the N_2O_2 coordination environment of a completely deprotonated $(L)^{4-}$ unit, and two μ-acetate groups bridge three metal(II) atoms. The distances

Table 2 Selected bond lengths (Å) and angles (°) of complexes **1**, **2** and **3**

Complex **1**		Complex **2**		Complex **3**	
Ca1–O1	2.650(3)	Sr1–O1	2.739(6)	Ba1–O1	2.845(8)
Ca1–O2	2.400(3)	Sr1–O2	2.531(5)	Ba1–O2	2.704(7)
Ca1–O5	2.398(3)	Sr1–O5	2.541(4)	Ba1–O5	2.667(6)
Ca1–O6	2.415(3)	Sr1–O6	2.533(4)	Ba1–O6	2.685(7)
Ca1–O9	2.382(3)	Sr1–O9	2.546(5)	Ba1–O9	2.716(7)
Ca1–O10	2.603(3)	Sr1–O10	2.745(5)	Ba1–O10	2.853(7)
Ca1–O11	2.389(4)	Sr1–O11	2.578(6)	Ba1–O11	2.719(7)
Ca1–O14	2.384(4)	Sr1–O14	2.549(5)	Ba1–O13	2.723(7)
O1–Ca1–O2	61.44(10)	O1–Sr–O2	59.29(16)	O1–Ba1–O2	56.7(2)
O1–Ca1–O5	121.72(10)	O1–Sr–O5	116.91(16)	O1–Ba1–O5	113.4(2)
O1–Ca1–O6	154.46(12)	O1–Sr–O6	146.68(18)	O1–Ba1–O6	145.8(2)
O1–Ca1–O9	105.92(11)	O1–Sr–O9	114.26(16)	O1–Ba1–O9	122.8(2)
O1–Ca1–O10	68.94(11)	O1–Sr–O10	79.05(19)	O1–Ba1–O10	89.2(2)
O1–Ca1–O11	76.33(11)	O1–Sr–O11	74.91(17)	O1–Ba1–O11	113.0(2)
O1–Ca1–O14	115.66(12)	O1–Sr–O14	116.62(19)	O1–Ba1–O13	79.5(2)
O2–Ca1–O5	66.06(10)	O2–Sr–O5	63.75(14)	O2–Ba1–O5	61.1(2)
O2–Ca1–O6	129.88(11)	O2–Sr–O6	123.40(15)	O2–Ba1–O6	118.3(2)
O2–Ca1–O9	164.52(11)	O2–Sr–O9	172.49(15)	O2–Ba1–O9	179.2(2)
O2–Ca1–O10	103.24(10)	O2–Sr–O10	114.11(15)	O2–Ba1–O10	123.5(2)
O2–Ca1–O11	104.01(12)	O2–Sr–O11	106.22(17)	O2–Ba1–O11	75.1(2)
O2–Ca1–O14	78.72(12)	O2–Sr–O14	77.27(17)	O2–Ba1–O13	108.0(2)
O5–Ca1–O6	63.85(10)	O5–Sr–O6	60.56(13)	O5–Ba1–O6	58.91(19)
O5–Ca1–O9	129.09(11)	O5–Sr–O9	123.74(14)	O5–Ba1–O9	119.1(2)
O5–Ca1–O10	149.29(13)	O5–Sr–O10	151.84(17)	O5–Ba1–O10	147.7(2)
O5–Ca1–O11	93.96(12)	O5–Sr–O11	97.83(18)	O5–Ba1–O11	69.1(2)
O5–Ca1–O14	75.14(12)	O5–Sr–O14	72.38(17)	O5–Ba1–O13	99.5(2)
O6–Ca1–O9	65.42(10)	O6–Sr–O9	64.05(14)	O6–Ba1–O9	61.7(2)
O6–Ca1–O10	120.48(11)	O6–Sr–O10	119.41(15)	O6–Ba1–O10	114.4(2)
O6–Ca1–O11	78.43(12)	O6–Sr–O11	72.80(17)	O6–Ba1–O11	95.8(2)
O6–Ca1–O14	89.85(12)	O6–Sr–O14	94.89(18)	O6–Ba1–O13	70.1(2)
O9–Ca1–O10	62.25(10)	O9–Sr–O10	59.29(14)	O9–Ba1–O10	56.8(2)
O9–Ca1–O11	79.89(12)	O9–Sr–O11	74.26(18)	O9–Ba1–O11	105.6(2)
O9–Ca1–O14	100.97(12)	O9–Sr–O14	103.93(17)	O9–Ba1–O13	71.2(2)
O10–Ca1–O11	116.74(12)	O10–Sr–O11	109.12(19)	O10–Ba1–O11	81.0(2)
O10–Ca1–O14	74.51(12)	O10–Sr–O14	79.74(18)	O10–Ba1–O13	107.5(2)
O11–Ca1–O14	166.76(12)	O11–Sr–O14	167.2(2)	O11–Ba1–O13	165.4(3)

Table 3 Hydrogen bonding interactions [Å °] for complexes **1**, **2** and **3**

D–H···A	d(D–H)	d(H···A)	d(*D*···A)	∠D–H···A	Symmetry
Complex 1					
C10–H10B···O13	0.97	2.37	3.308(6)	163	
C11–H11A···O13	0.97	2.60	3.433(7)	145	$2-x, -y, -z$
C18–H18···O3	0.93	2.37	3.195(6)	147	$-1+x, y, z$
C25–H25B···O12	0.97	2.60	3.524(6)	160	
Complex 2					
C1–H1B···O14	0.96	2.50	3.264(19)	137	
C10–H10A···O12	0.97	2.41	3.339(9)	160	
C22–H22···O8	0.93	2.47	3.233(9)	139	$-1+x, y, z$
C25–H25B···O13	0.97	2.46	3.380(10)	159	
Complex 3					
C1–H1C···O13	0.96	2.43	3.373(19)	167	
C10–H10B···O12	0.97	2.40	3.326(15)	160	
C21–H21···O8	0.93	2.48	3.251(13)	140	$1+x, y, z$
C25–H25B···O14	0.97	2.35	3.284(14)	160	
C33–H33A···O11	0.96	2.42	3.32(2)	156	

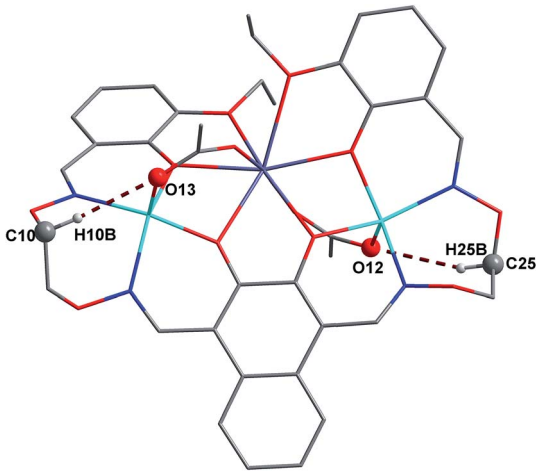

Fig. 4 View of the intramolecular hydrogen bonds of complex **1**.

between the two Zn(II) atoms (Zn1 and Zn2) and the four phenoxy oxygen atoms of the $(L)^{4-}$ unit range from 1.986(2) to 2.123(1) Å, and the distances between the Ca(II) atom and the four phenolic oxygen atoms (O2, O5, O6 and O9) on the $(L)^{4-}$ unit are 2.382(3) to 2.415(3) Å, which are shorter than the distances between the Ca(II) atoms and the ethoxy groups (Ca–O1 2.650(3) and Ca–O10 2.603(3)). The distances between the metal atoms and the coordination atoms indicate that the

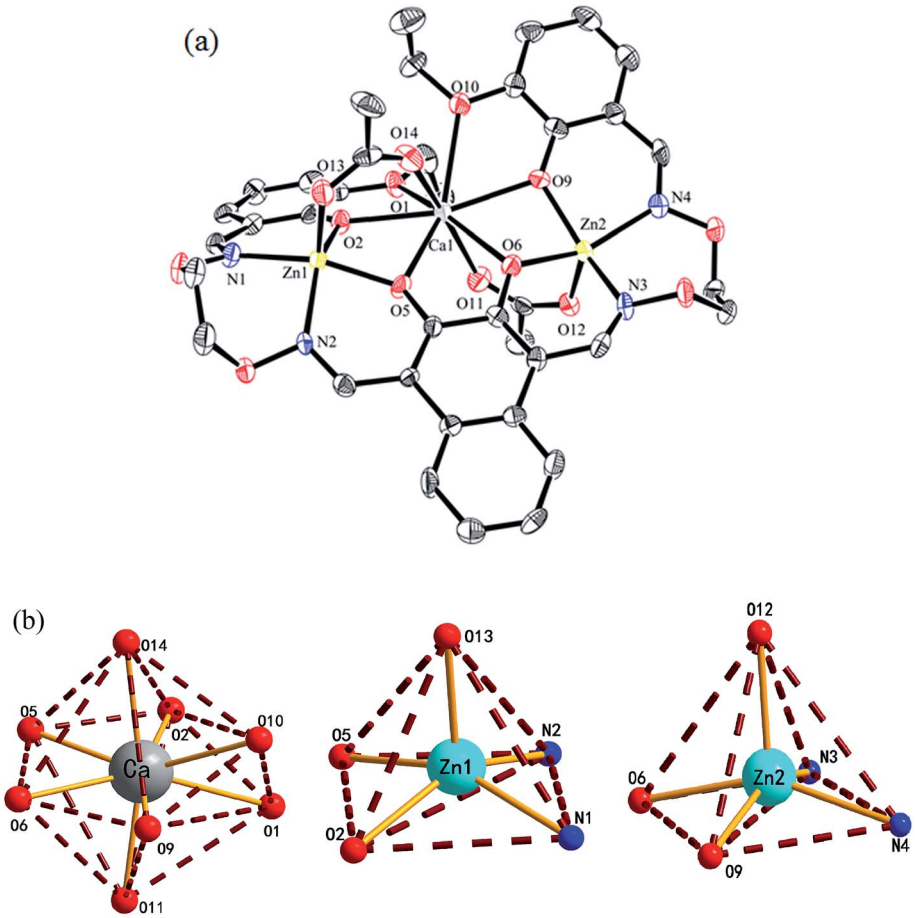

Fig. 3 (a) View of the molecular structure of complex **1** (hydrogen atoms and solvent molecules are omitted for clarity, and thermal ellipsoids are drawn at the 30% probability level). (b) Coordination polyhedra for the Zn(II) and Ca(II) atoms of complex **1**.

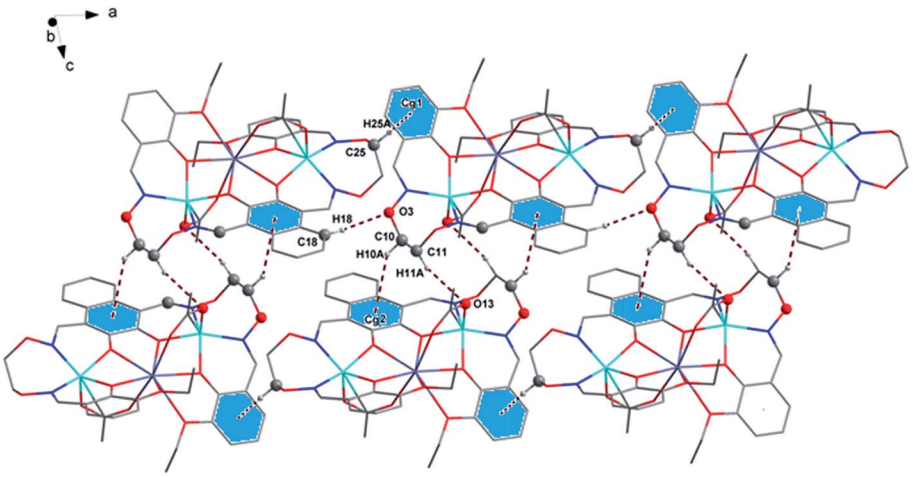

Fig. 5 View of an infinite 2D supramolecular network of complex **1**.

coordination cavity of the Ca(II) atom is larger than the coordination cavity in which the Zn1 and Zn2 atoms are located. The dihedral angles between the naphthalene ring and the two benzene rings are 44.88(4)° (C1–C6) and 11.96(4)° (C27–C32), respectively. The two μ-acetate groups are located on both sides of the naphthalene ring.

In complex **1**, the coordination pattern of the two Zn(II) atoms (Zn1 and Zn2) are penta-coordinated, and the τ values are 0.17 and 0.10,[18] respectively. Zn1 and Zn2 atoms both have distorted square pyramidal geometries,[19] while the central Ca(II) atom is octa-coordinated with a distorted square antiprism geometry.

In complex **1**, there are two intramolecular hydrogen bonds, C10–H10B···O13 and C25–H25B···O12.[20] As shown in Fig. 4, it is worth noting that the donor of both hydrogen bonds is located in the salamo unit and the receptors are oxygen atoms on the bridged μ-acetate groups. Thus, there are two kinds of intermolecular weak interactions existing in complex **1**. Among them, C25–H25A···Cg1 (C1–C2–C3–C4–C5–C6) and C10–H10A···Cg2 (C13–C14–C15–C16–C17–C18) form the intermolecular C–H···π interactions, and C18–H18···O3 and C11–H11A···O13 form the intermolecular C–H···O hydrogen bonds. As shown in Fig. 5, they finally form an infinite 2D supramolecular network along the *ac* plane.[21]

The crystal structures and atom numberings of complexes **2** and **3** are shown in Fig. S1 and S2,† respectively. The crystal structures of complexes **2** and **3** are similar to that of complex **1**. As shown in Fig. S3 and S4,† there are some intramolecular hydrogen bond interactions in complexes **2** and **3**. The infinite 2D supramolecular networks of complexes **2** and **3** are formed by abundant intermolecular C–H···O and C–H···π hydrogen bond interactions, as shown in Fig. S5 and S6.†

3.4 Fluorescence spectra

The fluorescence properties of H_4L and its corresponding complexes **1–3** were investigated at room temperature (Fig. 6). The ligand exhibits an intense emission peak at 508 nm. Compared with H_4L, the absorption peaks of complexes **1–3** are

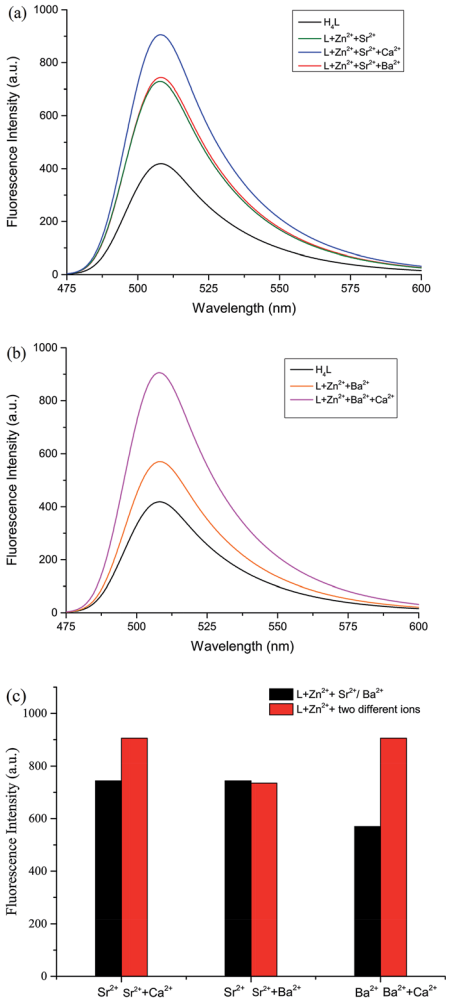

Fig. 6 (a) Fluorescence spectra of complex **2** solution (1.0×10^{-5} mol L^{-1}) in the absence and presence of various metal ions (1.0 equiv. of Ca(II) and Ba(II)). (b) Fluorescence spectra of complex **3** solution (1.0×10^{-5} mol L^{-1}) in the absence and presence of various metal ions (1.0 equiv. of Ca(II)). (c) Fluorescence response of L–Zn(II) solution (1.0×10^{-5} mol L^{-1}) to various metal ions. ex = 367 nm, em = 508 nm.

bathochromically-shifted, which is due to the intraligand π–π* transition.[22] It is obvious that the Ca(II), Sr(II) and Ba(II) enhance the fluorescence intensity. In order to explore the differences in coordination capabilities of Ca(II), Sr(II) and Ba(II) ions, ion competitive experiments were investigated, as shown in Fig. 6. We have studied the fluorescence changes of complex **2** solution (1.0×10^{-5} mol L^{-1}) in the presence of Ca(II) and Ba(II), respectively. As shown in Fig. 6(a), a dramatic increase in emission intensity is induced by the addition of Ca(II) to the Sr(II) complex solution, suggesting that the Sr(II) is replaced by Ca(II). When Ba(II) was added, the fluorescence intensity showed no change, indicating that the coordination ability of Sr(II) was stronger than that of Ba(II). Similarly, as shown in Fig. 6(b), when Ca(II) was added to the solution of complex **3** (1.0×10^{-5} mol L^{-1}), the fluorescence intensity increased sharply, indicating that the coordination ability of Ca(II) was stronger than that of Ba(II). As a result, the coordinating capability in the central O_6 site is in the order of Ca(II) > Sr(II) > Ba(II).

4. Conclusion

Three heteronuclear Zn(II)–M(II) (M = Ca, Sr and Ba) complexes with a naphthalenediol-based bis(salamo)-type tetraoxime ligand H_4L were designed and synthesized. The fluorescence spectra of complexes **1**, **2** and **3** were also studied. The coordination ratio of Zn(II) to H_4L was 2 : 1, and that of M(II) (M = Ca, Sr and Ba) to H_4L was 1 : 1. X-ray crystal structures reveal that the different natures of the N_2O_2 and O_6 sites of H_4L lead to the site-selective introduction of two different kinds of metal(II) atoms. The coordination numbers of Ca(II), Sr(II) and Ba(II) atoms in the O_6 environment are all 8, and they have slightly distorted square antiprism geometries. As a result, the coordinating capability in the central O_6 site is in the order of Ca(II) > Sr(II) > Ba(II). The supramolecular structures of complexes **1**, **2** and **3** are formed *via* intermolecular C–H···O and C–H···π hydrogen bond interactions, leading to a self-assembly infinite 2D network structure.

Conflicts of interest

There are no conflicts to declare.

Acknowledgements

This work was supported by the National Natural Science Foundation of China (21361015 and 21761018) and the Program for Excellent Team of Scientific Research in Lanzhou Jiaotong University (201706), which are gratefully acknowledged.

References

1 (*a*) S. S. Sun, C. L. Stern, S. T. Nguyen, J. T. Hupp and J. T. Hupp, *J. Am. Chem. Soc.*, 2004, **126**, 6314–6326; (*b*) L. Zhao, X. T. Dang, Q. Chen, J. X. Zhao and L. Wang, *Synth. React. Inorg., Met.-Org., Nano-Met. Chem.*, 2013, **43**, 1–6; (*c*) L. Zhao, L. Wang, Y. X. Sun, W. K. Dong, X. L. Tang and X. H. Gao, *Synth. React. Inorg., Met.-Org., Nano-Met. Chem.*, 2012, **42**, 1303–1308; (*d*) P. Wang and L. Zhao, *Spectrochim. Acta, Part A*, 2015, **135**, 342–350; (*e*) Y. X. Sun, S. T. Zhang, Z. L. Ren, X. Y. Dong and L. Wang, *Synth. React. Inorg., Met.-Org., Nano-Met. Chem.*, 2013, **43**, 995–1000; (*f*) X. Y. Dong, Y. X. Sun, L. Wang and L. Li, *J. Chem. Res.*, 2012, **36**, 387–390; (*g*) Y. X. Sun and X. H. Gao, *Synth. React. Inorg., Met.-Org., Nano-Met. Chem.*, 2011, **41**, 973–978; (*h*) Y. X. Sun, L. Xu, T. H. Zhao, S. H. Liu, G. H. Liu and X. T. Dong, *Synth. React. Inorg., Met.-Org., Nano-Met. Chem.*, 2013, **43**, 509–513.

2 (*a*) H. L. Wu, Y. C. Bai, Y. H. Zhang, Z. Li, M. C. Wu, C. Y. Chen and J. W. Zhang, *J. Coord. Chem.*, 2014, **67**, 3054–3066; (*b*) C. Y. Chen, J. W. Zhang, Y. H. Zhang, Z. H. Yang, H. L. Wu, G. L. Pan and Y. C. Bai, *J. Coord. Chem.*, 2015, **68**, 1054–1071; (*c*) H. L. Wu, G. L. Pan, Y. C. Bai, Y. H. Zhang, H. Wang, F. R. Shi, X. L. Wang and J. Kong, *J. Photochem. Photobiol., B*, 2014, **135**, 33–43; (*d*) H. L. Wu, H. Wang, X. L. Wang, G. L. Pan, F. R. Shi, Y. H. Zhang, Y. C. Bai and J. Kong, *New J. Chem.*, 2014, **38**, 1052–1061; (*e*) H. L. Wu, G. L. Pan, Y. C. Bai, H. Wang, J. Kong, F. R. Shi, Y. H. Zhang and X. L. Wang, *J. Coord. Chem.*, 2013, **66**, 2634–2646.

3 (*a*) T. K. Chin, S. Endud, S. Jamil, S. Budagumpi and H. O. Lintang, *Catal. Lett.*, 2013, **143**, 282–288; (*b*) X. Y. Li, L. Chen, L. Gao, Y. Zhang, S. F. Akogun and W. K. Dong, *RSC Adv.*, 2017, **7**, 35905–35916.

4 (*a*) W. K. Dong, J. C. Ma, Y. J. Dong, L. C. Zhu and Y. Zhang, *Polyhedron*, 2016, **115**, 228–235; (*b*) P. P. Liu, L. Sheng, X. Q. Song, W. Y. Xu and Y. A. Liu, *Inorg. Chim. Acta*, 2015, **434**, 252–257; (*c*) X. Q. Song, P. P. Liu, Z. R. Xiao, X. Li and Y. A. Liu, *Inorg. Chim. Acta*, 2015, **438**, 232–244; (*d*) Y. A. Liu, C. Y. Wang, M. Zhang and X. Q. Song, *Polyhedron*, 2017, **127**, 278–286.

5 (*a*) L. Q. Chai, G. Wang, Y. X. Sun, W. K. Dong, L. Zhao and X. H. Gao, *J. Coord. Chem.*, 2012, **65**, 1621–1631; (*b*) L. Q. Chai, J. J. Huang, H. S. Zhang, Y. L. Zhang, J. Y. Zhang and Y. X. Li, *Spectrochim. Acta, Part A*, 2014, **131**, 526–533; (*c*) L. Q. Chai, G. Liu, J. Y. Zhang, J. J. Huang and J. F. Tong, *J. Coord. Chem.*, 2013, **66**, 3926–3938; (*d*) L. Q. Chai, L. J. Tang, L. C. Chen and J. J. Huang, *Polyhedron*, 2017, **122**, 228–240; (*e*) L. Q. Chai, K. Y. Zhang, L. J. Tang, J. Y. Zhang and H. S. Zhang, *Polyhedron*, 2017, **130**, 100–107.

6 (*a*) Y. J. Dong, X. Y. Dong, W. K. Dong, Y. Zhang and L. S. Zhang, *Polyhedron*, 2017, **123**, 305–315; (*b*) W. K. Dong, J. C. Ma, Y. J. Dong, L. Zhao, L. C. Zhu, Y. X. Sun and Y. Zhang, *J. Coord. Chem.*, 2016, **69**, 3231–3241; (*c*) H. L. Wu, C. P. Wang, F. Wang, H. P. Peng, H. Zhang and Y. C. Bai, *J. Chin. Chem. Soc.*, 2015, **62**, 1028–1034.

7 (*a*) W. K. Dong, J. C. Ma, L. C. Zhu, Y. Zhang and X. L. Li, *Inorg. Chim. Acta*, 2016, **445**, 140–148; (*b*) S. Ömer, Ö. Ö. Ümmühan, S. Nurgul, A. Burcu, S. Musa, T. Tuncay and S. Zeynel, *Tetrahedron*, 2016, **72**, 5843–5852.

8 (*a*) W. K. Dong, X. L. Li, L. Wang, Y. Zhang and Y. J. Dong, *Sens. Actuators, B*, 2016, **229**, 370–378; (*b*) W. K. Dong,

S. F. Akogun, Y. Zhang, Y. X. Sun and X. Y. Dong, *Sens. Actuators, B*, 2017, **238**, 723–734; (*c*) B. J. Wang, W. K. Dong, Y. Zhang and S. F. Akogun, *Sens. Actuators, B*, 2017, **247**, 254–264; (*d*) L. M. Pu, S. F. Akogun, X. L. Li, H. T. Long, W. K. Dong and Y. Zhang, *Polyhedron*, 2017, **134**, 356–364.

9 (*a*) S. Akine, T. Taniguchi and T. Nabeshima, *Inorg. Chem.*, 2008, **47**, 3255–3264; (*b*) S. Akine, T. Taniguchi, T. Saiki and T. Nabeshima, *J. Am. Chem. Soc.*, 2005, **127**, 540–541; (*c*) S. Akine, T. Taniguchi and T. Nabeshima, *J. Am. Chem. Soc.*, 2006, **128**, 15765–15774.

10 S. Akine, T. Taniguchi, W. K. Dong, S. Masubuchi and T. Nabeshima, *J. Org. Chem.*, 2005, **70**, 1704–1711.

11 (*a*) X. Y. Dong, S. F. Akogun, W. M. Zhou and W. K. Dong, *J. Chin. Chem. Soc.*, 2017, **64**, 412–419; (*b*) Y. J. Dong, X. L. Li, Y. Zhang and W. K. Dong, *Supramol. Chem.*, 2017, **29**, 518–527; (*c*) W. K. Dong, J. Zhang, Y. Zhang and N. Li, *Inorg. Chim. Acta*, 2016, **444**, 95–102; (*d*) W. K. Dong, G. Li, Z. K. Wang and D. X. Yong, *Spectrochim. Acta, Part A*, 2014, **133**, 340–347.

12 (*a*) L. Chen, W. K. Dong, H. Zhang, Y. Zhang and Y. X. Sun, *Cryst. Growth Des.*, 2017, **17**, 3636–3648; (*b*) W. K. Dong, S. S. Zheng, J. T. Zhang, Y. Zhang and Y. X. Sun, *Spectrochim. Acta, Part A*, 2017, **184**, 141–150; (*c*) S. S. Zheng, W. K. Dong, Y. Zhang, L. Chen and Y. J. Ding, *New J. Chem.*, 2017, **41**, 4966–4973.

13 (*a*) S. Akine, T. Tadokoro and T. Nabeshima, *Inorg. Chem.*, 2012, **51**, 11478–11486; (*b*) S. Akine, S. Sairenji, T. Taniguchi and T. Nabeshima, *J. Am. Chem. Soc.*, 2013, **135**, 12948–12951; (*c*) H. A. Tran, J. Collins and P. E. Georghiou, *New J. Chem.*, 2008, **32**, 1175–1182.

14 G. M. Sheldrick, *SHELXS 97, Program for crystal structure solution*, University of Göttingen, Göttingen, Germany, 1997.

15 G. M. Sheldrick, *SHELXL 97, Program for crystal structure refinement*, University of Göttingen, Göttingen, Germany, 1997.

16 Y. J. Dong, J. C. Ma, L. C. Zhu, W. K. Dong and Y. Zhang, *J. Coord. Chem.*, 2017, **70**, 103–115.

17 (*a*) L. Xu, L. C. Zhu, J. C. Ma, Y. Zhang, J. Zhang and W. K. Dong, *Z. Anorg. Allg. Chem.*, 2015, **641**, 2520–2524; (*b*) W. K. Dong, J. T. Zhang, Y. J. Dong, Y. Zhang and Z. K. Wang, *Z. Anorg. Allg. Chem.*, 2016, **642**, 189–196; (*c*) W. K. Dong, J. C. Ma, L. C. Zhu, Y. X. Sun, S. F. Akogun and Y. Zhang, *Cryst. Growth Des.*, 2016, **16**, 6903–6914.

18 (*a*) A. W. Addison, T. N. Rao, J. Reedijk, J. van Rijn and G. C. Verschoor, *J. Chem. Soc., Dalton Trans.*, 1984, **7**, 1349–1356; (*b*) T. Konno, K. Tokuda, J. Sakurai and K. I. Okamoto, *Bull. Chem. Soc. Jpn.*, 2000, **73**, 2767–2773.

19 G. L. Paraginski, M. Hörner, D. F. Back and J. Beck, *J. Mol. Struct.*, 2016, **1104**, 79–84.

20 (*a*) L. Zhao, X. T. Dang, Q. Chen, J. X. Zhao and L. Wang, *Synth. React. Inorg., Met.-Org., Nano-Met. Chem.*, 2013, **43**, 1241–1246; (*b*) L. Q. Chai, Y. X. Li, L. C. Chen, J. Y. Zhang and J. J. Huang, *Inorg. Chim. Acta*, 2016, **444**, 193–201; (*c*) Y. X. Sun, C. Y. Li, C. J. Yang, Y. Y. Zhao, J. Q. Guo and B. Yu, *Chin. J. Inorg. Chem.*, 2016, **32**, 327–335; (*d*) Y. X. Sun, L. Wang, X. Y. Dong, Z. L. Ren and W. S. Meng, *Synth. React. Inorg., Met.-Org., Nano-Met. Chem.*, 2013, **43**, 599–603.

21 (*a*) P. Wang and L. Zhao, *Synth. React. Inorg., Met.-Org., Nano-Met. Chem.*, 2016, **46**, 1095–1101; (*b*) Y. X. Sun, Y. Y. Zhao, C. Y. Li, B. Yu, J. Q. Guo and J. Li, *Chin. J. Inorg. Chem.*, 2016, **32**, 913–920; (*c*) L. Q. Chai, K. H. Mao, J. Y. Zhang, K. Y. Zhang and H. S. Zhang, *Inorg. Chim. Acta*, 2017, **457**, 34–40; (*d*) L. Q. Chai, J. J. Huang, J. Y. Zhang and Y. X. Li, *J. Coord. Chem.*, 2015, **68**, 1224–1237; (*e*) X. Q. Song, G. Q. Cheng, X. R. Wang, W. Y. Xu and P. P. Liu, *Inorg. Chim. Acta*, 2015, **425**, 145–153.

22 W. K. Dong, J. C. Ma, L. C. Zhu, Y. X. Sun, S. F. Akogun and Y. Zhang, *New J. Chem.*, 2016, **40**, 6998–7010.